THIRTEENTH EUROPEAN ROTORCRAFT FORUM

6.11

Paper No. 103

FURTHER EXPERIENCE WITH A NEW APPROACH TO HELICOPTER AEROELASTICITY

G T S Done (City University, London, UK)
P T W Juggins (Westland Helicopters Ltd., Yeovil, UK)
M H Patel (Garrad-Hassan Ltd., London, UK)

September 8-11, 1987

ARLES, FRANCE

ASSOCIATION AERONAUTIQUE ET ASTRONAUTIQUE DE FRANCE

FURTHER EXPERIENCE WITH A NEW APPROACH TO HELICOPTER AEROELASTICITY

by

G T S Done (City University, London, UK)
P T W Juggins (Westland Helicopters Ltd., Yeovil, UK)
M H Patel (Garrad-Hassan Ltd., London, UK)

Abstract

Further experience with an alternative procedure for computing the aeroelastic stability of a helicopter is described. The basic method has been previously presented and is aimed at generating the coefficients of the aeroelastic equations of motion automatically on the computer. A series of exercises has been undertaken with the objective of verifying the computer program and the first group of these has been previously reported. This paper describes the remaining exercises, and covers air resonance in forward flight, transmission system and fuselage flexibility, and non-homogeneity of the main rotor control jack stiffnesses.

1. Introduction

A method which allows much of the tedious algebraic manipulation required when formulating aeroelastic equations of motion to be effectively performed instead by the computer has already been described [1]. Experience with this alternative method, based on a programme of three initial verification exercises, has similarly also been presented [2].

The method is embodied in a computer program called AGEM (Automatic Generation of Equations of Motion). In the program, the position of a material point on the system under investigation, which in the present paper is a helicopter or part of a helicopter, is described in terms of mode shapes and transformation matrices, the latter relating one set of co-ordinate axes to another. The program performs numerically all integrations and differentiations, including those required in the Lagrange equations formulation. The equations of motion themselves are implied from the computed coefficients and apply to perturbation co-ordinates linearised about an equilibrium state. A condensed version of the relevant mathematics is reproduced in Appendices A.1 and A.2.

This computer based method is not designed necessarily to increase insight or lead to extra understanding of the factors important in helicopter aeroelasticity. These can be more than amply obtained by studying reviews such as those of Friedmann [3, 4] and the various papers reviewed therein. The method should be compared with approaches such as GRASP (see Hodges et al [5]) or those using symbolic computing (see for example Garrad and Quarton [6]).

The previous verification exercises were aimed at testing specific parts of the program and are fully described in Ref [2]. The exercises presented in this paper complete the programme of verfication tests that were originally devised to build up

confidence in the use of AGEM. They are based on air resonance models of the Westland Lynx helicopter (in forward flight) and of a bearingless main rotor experimental model for which stability data already existed. Further studies include the incorporation of transmission system and flexible fuselage dynamics into the computer model, as well as the effects of non-homogeneity in the (non- rotating) rotor control jack stiffnesses.

For verification purposes, in each case the AGEM model was set up exactly in the manner of previous analysis by WHL, so that the initial data, the order of the various transformations and general mathematical modelling were maintained. The results are presented and discussed in the following sections.

2. Verification Exercises

2.1 Lynx air resonance in forward flight

A mathematical model of the WHL Lynx has previously been derived by dynamicists in a conventional manner, and the results of an air resonance stability analysis were available. These provided the basis for a verification exercise in which the computer program AGEM was used to derive the relevant equations of motion and produce results for comparison with those previously obtained. The form of the model used was therefore defined by the original Westland analysis.

The air resonance model is shown diagrammatically in Fig 1. It comprises 16 degrees of freedom. Five of these are rigid body fuselage motions, namely, fore-and-aft and sideways translation, heave, roll and pitch. Each of the four blades has two degrees of freedom, being represented by previously determined mode shapes in "pure" flap and lag and including δ_3 and α_2 coupling. The remaining three degrees of freedom arise from the incorporation into the model of a representation of the autostabilisation equipment (ASE).

The general treatment and presentation of model data remains largely as in Refs [1] and [2]. However, it has since been necessary to incorporate into AGEM some additional facilities in order to use it on the current problem, the introduction of the ASE being a case in point; another example involves fuselage aerodynamics.

Some further details of these and other relevant contributory factors are given below, followed by a comparison of results.

2.1.1. Rotor blade aerodynamics

The treatment of the blade aerodynamics is as described in Ref [1]. Strip theory is used, the aerodynamic forces being dependent on section lift, drag and moment coefficients. The latter contains a component that is dependent on section pitching velocity. The induced velocity is defined normal to the tip path plane, which in turn is given by the steady state cyclic flapping inputs. These, and other steady state trim data are assumed to be

already provided by other computer programs. The actual induced velocity distribution within the rotor disc whilst in forward flight is based on Glauert (see Bramwell [7]), so that there is a cyclic component. There are also incorporated additional components of induced velocity that result from perturbatory rigid body motions of the fuselage.

2.1.2. Fuselage aerodynamics

The contributions to the equations of motion are formed within AGEM via the appropriate scalar products in equations (A.1.3) and (A.1.4) of Appendix 1, namely, those containing the vector $\underset{\sim}{F}$ which is the aerodynamic force vector per unit area referred to space fixed axes. The manner in which $\underset{\sim}{F}$ is formulated from the fuselage aerodynamic data is very similar to that described in Ref [1] in connection with rotor blade aerodynamic terms; this involves rotational transformations between space fixed axes and axes fixed in the body, which in this case is the fuselage.

The fuselage aerodynamic data are provided at a specified steady flight condition and consist of a vector of steady force and moment components, and a (5×5) matrix of derivatives. The latter provides the contribution to the former resulting from five† perturbations of the fuselage in the rigid body directions. The velocity perturbations (corresponding to fore-and-aft, sideways and heave motions) are initially resolved such that they are relative to the fuselage principal axes. The scalar products referred to above are formed in a similar way to that outlined in Section 4.2.1. of Ref [1].

2.1.3. Autostabilisation control system equations

The aircraft stability is enhanced by the autostabilisation equipment (or ASE). The control is effected by providing additional blade pitch deflections that are certain functions of the aircraft attitude in roll and pitch, and the aircraft vertical acceleration. The overall contribution to the blade pitch from the ASE, θ_{AS}, is given by

$$\theta_{AS} = \theta_{\phi} \cos\Upsilon_k + \theta_{\psi} \sin\Upsilon_k + \theta_z \qquad (2.1)$$

where θ_{ϕ} and θ_{ψ} are the blade pitch contributions from fuselage roll and pitch respectively, θ_z is the contribution from the collective acceleration control (CAC), and Υ_k is the azimuthal angle of the kth blade measured from the front of the disc.

The three degrees of freedom introduced by the ASE are thus effectively θ_{ϕ}, θ_{ψ} and θ_z, and these are related to the aircraft attitudes and motions in roll, pitch and heave by the following set of equations.

$$K_{2j}\ddot{\theta}_j + K_{1j}\dot{\theta}_j + K_{0j}\theta_j + G_{2j}\ddot{q}_j + G_{1j}\dot{q}_j\, G_{0j}q_j = 0 \qquad (2.2)$$

† yaw excluded

in which suffix j= ϕ, ψ or z, and some of the coefficients K_{ij} or G_{ij} may be zero. Additionally, some parts of the contributions from the fuselage rigid body roll and pitch are subject to imposed constraints.

These equations are presented in such a way as to indicate in a direct fashion the coupling between the blade pitch contributions and the overall aircraft motions. The actual determination of the various constants follows from a detailed analysis of the various component parts and control systems that make up the autostabilisation equipment, and is not presented here.

2.1.4. Comparison of results

The equations of motion for the air resonance model in forward flight have periodic coefficients, and are solved via the Floquet method. An efficient numerical technique is used, and use is also made of the symmetry of the rotor, in order to reduce computation time. The blade mass is modelled in a simple manner by concentrating its distribution along a single line within the blade, and this also helps to minimise the computation time.

For a particular forward flight speed, the real and imaginary parts of the eigenvalues from AGEM are shown compared with those previously obtained by WHL in Table 1. There are small differences here and there but they are not really significant. The overall result is to provide confidence in the program.

Another element of the verification consisted of obtaining the coefficient matrices at a particular instant of flight. Thus, the inertia, damping and stiffness matrices were obtained from the program at the instant when the forward pointing blade was 6 degrees off the fore-and-aft axis, and compared with those obtained by WHL. This implied comparing some 300 pairs of numbers (excluding zeroes and symmetric elements) of greatly varying magnitude, and it is not considered useful to reproduce the matrix coefficients here. Suffice it to say that the comparison between the two sets was very largely excellent, and again provided further confidence in the computer program.

2.2. Bearingless main rotor model

2.2.1. Comparison with test results

Measurement of the ground and air resonance stability of a model bearingless main rotor, as reported in Ref. [8] has been performed in order to substantiate analytical prediction methods. Comparisons were made with predictions from a WHL stability analysis which uses "pure" components of flap and lag modes as degrees of freedom, together with pitch-lag and pitch-flap coupling coefficients, obtained from fully-coupled modes predicted by a WHL blade modes analysis.

AGEM can be applied in the same manner as the WHL stability analysis (i.e. using "pure" modes), and good correlation between

the two analyses has been demonstrated, as reported in Ref [2] and the first verification exercise above. This good correlation was also obtained for predictions of stability for the model bearingless rotor.

A further facility of the AGEM program is its application with fully coupled blade modes as the degrees of freedom. Inital comparisons were made between predictions using this facility and the test results for the model bearingless rotor. These comparisons showed a rather poor level of agreement.

In considering the reasons for this, an important factor was identified as the method of modelling the torque tube used to apply blade pitch control. The torque tube is represented in the WHL blade modes analysis as a second flexural load path adjacent to the main hub flexure element, with an impedance model of the control system. This load path is fully described in terms of its geometry and distribution of section inertia and stiffness properties. The initial configuration of the AGEM program was written to model a single load path, with a control system stiffness model. In the coupled modes application of the program, contributions arising from motion of the torque tube might not therefore be adequately modelled.

2.2.2. Investigation of modelling techniques - the torque tube

In order to investigate further the significance of the method of torque tube modelling, as well as effects of other modelling assumptions, a series of comparisons were made between calculated eigenvalues for a single blade hub-fixed configuration, using a WHL coupled modes stability program and the AGEM program, incorporating the first flap, lag and torsion modes.

The WHL analysis used the fully coupled modes from the blade modes program as degrees of freedom, as well as mass, stiffness and damping matrix terms calculated within that program due to inertial or structural stiffness effects, including those for the torque tube. In this way the very fine integration step length of the modes program was utilised for these terms. Additionally, a quasi-steady aerodynamic model was applied in the stability program.

Eigenvalue results for the WHL program and the AGEM program are shown in Fig 2 for two standards of AGEM model. Case 1 is the result from the WHL program. In Case 2 the AGEM model includes no representation of the torque tube apart from that implicit in control system deflections. In Case 3 a lumped inertia representation of the torque tube is included, with the inertia value calculated as that which would give good correlation of torsion frequency with no aerodynamic effects present.

The results show some large differences between Case 1 and the AGEM calculations. The inclusion of the torque tube inertia model can be seen to give some improvement in agreement of flap and torsion frequencies, although the lag damping agreement is degraded. A conclusion could be made that the level of torque

tube representation in cases 2 and 3 was inadequate. In order to support this conclusion further comparisons of fixed-hub stability predictions were made, for a rotor with no torque tube.

2.2.3. Other modelling technique effects

Comparisons between fixed-hub stability predictions for a Sea King tail rotor, using the AGEM program and a WHL analysis are reported in Ref [2]. In that case a hinged rigid blade representation was employed, and correlation was good.

More recent further comparisons for fixed-hub blade stability were made using the AGEM program and the WHL coupled modes stability program, as applied in the torque tube modelling exercise, above. The further comparisons were made for blade data representing a Lynx-type semi-rigid rotor, but with smoothed section property distributions and assumed control system stiffness and geometry to give a large magnitude of pitch-flap and pitch-lag coupling. Calculated eigenvalues for this "theoretical" rotor are shown in Fig 3 for three different AGEM models and the WHL analysis.

Case 1 is the calculation from the WHL program. Case 2 is an AGEM representaiton with few input points around the point of attachment of the control system load path. Cases 3 and 4 have more input points around this point, but in Case 3 the blade structural stiffness matrix is calculated within the AGEM program, while in Case 4 it is input from the WHL blade modes program.

It should be noted that the AGEM calculations uses the blade modes and properties defined at 25 radial points, while for non-aerodynamic terms the WHL analysis definition is effectively at 900 points (the integration steps of the blade modes program).

It can be seen that overall correlation between all cases is good. Case 2 exhibits a degraded correlation in flap frequency with Case 1, while Case 3 exhibits a degraded correlation of lag damping. Differences between calculations from the AGEM models are often greater than their individual differences when compared with Case 1.

The conclusion from this study is that, while correlation is good, care is required in using the AGEM program in the choice of input points in relationship to load path branches and also to significant discontinuities in section properties. In addition the structural stiffness matrix should ideally be calculated within the blade modes program.

2.2.4. Twin load path representation

Subsequent to these studies, inclusion of representation of the bearingless rotor torque tube as a second flexural load path in the AGEM program is proceeding.

3. Fuselage and transmission system flexibility

The underlying analysis for AGEM is essentially modal in approach; if the instantaneous position in space of a point on a component part of a helicopter can be expressed by means of modal expressions, and rotational and translational transformations, then that component part can be incorporated into the helicopter model. The incorporation of the transmission system dynamics and/or the fuselage dynamics (beyond straightforward rigid body motions) represents no special difficulty.

3.1. Transmission system

The mechanical transmission system, comprising the gearbox, engines, tail rotor and other ancillary rotating equipment is modelled by means of a number of previously computed normal modes. It is connected to the rotor at the rotorhead, and thus the modal deflections at this end of the transmission model are used to provide the rotational transformation matrix

$$\left[T_{\gamma T}\right] = \begin{bmatrix} \cos\gamma_T & -\sin\gamma_T & 0 \\ \sin\gamma_T & \cos\gamma_T & 0 \\ 0 & 0 & 1 \end{bmatrix} \qquad (3.1)$$

at the rotor axis. This is inserted at the appropriate positions in equation (A.2.3). The angle $\gamma_T = \sum_i f_{Ti}\, q_i$, in which f_{Ti} is the modal angular deflection at the rotor end of the transmission in the ith mode. It is usually convenient to define the modal deflections such that a unit generalised mass matrix is produced, the stiffness matrix then being a diagonal matrix of natural frequencies squared.

The transmission system for the Lynx had been previously analysed by WHL using a lumped parameter, multi-branch model comprising 48 components reducing to a 22 d.o.f. model. Results both for the system including a representation of the main rotor having three lag modes per blade, and for the system excluding the main rotor were available, and these formed the basis for a verification exercise.

The latter results were used to provide the six lowest frequency transmission modes, and these were used in AGEM with eight rotor blade modes, comprising the lowest two "pure" lag bending modes per blade. The rotor was running at normal operating speed and aerodynamic forces were absent. The eigenvalues were found and the lowest six of these (bar the rigid body mode zero frequency) are shown compared in Table 2 with the results obtained from the former of Westland analyses mentioned above.

The lower frequencies compare fairly well but the poorer comparison at the higher frequency end is considered due to the smaller number of degrees of freedom used in the AGEM model.

3.2. Flexible fuselage

The incorporation of a rigid fuselage into the overall model, as in the air resonance exercise described in Section 2.1, requires the input of the appropriate mass and inertia data, centre of mass geometry, and rotational transformation matrices, as in equation (A, 2, 3). When the fuselage is flexible, a point on the fuselage is additionally described by modal displacements, and there are also generalised mass and stiffness contributions to the equations of motion. Furthermore, the rotor axis can be considered attached to that part of the fuselage adjacent to the rotor head, and so the rotational and translational transformation matrices that apply to the rotor axis contain elements arising from the modal deformations of the fuselage in this region.

The rotational transformation matrices are exactly similar to that in equation (3. 1), and there are three, corresponding to the three rotation axes possible. The angle in the pitching sense transformation matrix is $\sum_i f_{F\phi i}\, q_i$, for example, in which $f_{F\phi i}$ is the modal pitch deflection at the rotor head position on the fuselage in the ith mode. Similar expressions appear for roll and yaw, and indeed also for the three translational deflections. The latter, and the rotational transformation matrices are inserted into the appropriate positions in equation (A.2.3.).

The incorporation of flexible fuselage dynamics into the AGEM could not be properly verified, due to lack of results obtained by some other means. However, data existed for a free-free fuselage model of the Lynx which carried a lumped mass and inertia representation of the main rotor. These data allowed six normal modes having substantial hub motion to be selected. These modes were used in an AGEM model which also comprised eight rotor modes, that is, fundamental flap and lag modes for each of the four blades. The rotor ran at normal operating speed and blade aerodynamics were excluded. For simplicity, rigid body motions of the fuselage were suppressed.

Natural frequencies for this simplistic model were obtained, and those that can be identified with the natural frequencies of the initial fuselage model are shown with the latter for comparison in Table 3. Five of the six fuselage modal frequencies can still be identified, but the change in natural frequency as a result of the coupling is generally not significant.

4. Control jack flexibility

In Ref [2] the effect of the flexibilities of the control jacks was introduced in a simple way by replacing each blade pitch control rod by a spring having one end grounded. Both flap and pitch motions are affected due to the geometrical offsets of the pitch control rod mounting point from the blade and rotation axes.

In the present exercise this model is improved and made more representative by placing the (flexible) control jacks below the swash plate, assuming that this type of control applies, and making the blade pitch control rods infinitely stiff. If the lower (non-rotating) part of the swash plate were mounted on a

perfectly homogeneous stiffness, the model would in effect be no different dynamically from the former simpler model (leaving aside consideration of the mass of the various components, for the moment). However, the actual configuration and the ratings of the jacks generally give rise to a non-homogeneous stiffness, which as far as a rotating blade is concerned, is felt as a periodic structural stiffness acting in pitch and flap.

The following analysis shows how the stiffness contributions are obtained.

4.1. Control jack stiffness contributions

Fig. 4 shows a swashplate control arrangement in which the control jacks are attached at points 1, 2 and 3. When the jacks move the lower part of the swashplate away from the datum position, the cylindrical co-ordinates of the jack mounting points are given by $\{r_i, \Upsilon_i, \delta_i\}$, $i = 1, 2, 3$, as shown in the Figure. The equation of the plane containing points 1, 2, and 3 is given by

$$\underset{\sim}{\delta} = \underset{\sim}{F}\,\underset{\sim}{p} \qquad (4.1)$$

in which

$$\underset{\sim}{F} = \begin{bmatrix} 1 & r_1\cos\Upsilon_1 & r_1\sin\Upsilon_1 \\ 1 & r_2\cos\Upsilon_2 & r_2\sin\Upsilon_2 \\ 1 & r_3\cos\Upsilon_3 & r_3\sin\Upsilon_3 \end{bmatrix}$$

$$\underset{\sim}{\delta} = \{\delta_1, \delta_2, \delta_3\}$$

and $\underset{\sim}{p} = \{p_1, p_2, p_3\}$ is a vector of three equation coefficients. This describes the instantaneous position of the lower (non-rotating) part of the swashplate. The upper (rotating) part is assumed to lie in the same plane, and it too may be described in a similar way through the deflections e_{ja} of the lower ends of the pitch control rods, where $j = 1, 2, \ldots N$, and N is the number of blades.

For clarity, only blade number 1 is shown in Fig. 4. Thus

$$e_{ja} = p_1 + r_p\left\{p_2\cos\left[\Upsilon + 2(j-1)\frac{\pi}{N}\right] + p_3\sin\left[\Upsilon + 2(j-1)\frac{\pi}{N}\right]\right\} \qquad (4.2)$$

in which p_1, p_2, and p_3 are the equation coefficients as before, and the radius of the pitch control rods, r_p, is assumed the same for each blade. This provides

$$\underset{\sim}{e}_A = \underset{\sim}{G}(\Upsilon)\underset{\sim}{p}$$

$$= \underset{\sim}{G}\underset{\sim}{F}^{-1}\underset{\sim}{\delta} \qquad (4.3)$$

from equation (4.1), in which $\underset{\sim}{e}_A \equiv \{\underset{\sim}{e}_{1A}\ \underset{\sim}{e}_{2A}\ \ldots\ldots\}$. Thus, the pitch control rod deflections are given by three independent variables, δ_1, δ_2, and δ_3.

However, these deflections can also be expressed in terms of the flapping and pitching deflections of each blade, via knowledge of the associated mode shapes and pitching moment aim geometry. This may be expressed as

$$\underset{\sim}{e}_B = \underset{\sim}{A}\,\underset{\sim}{q} \qquad (4.4)$$

in which $\underset{\sim}{q}$ is a vector containing all relevant blade generalised co-ordinates. The number of dependent variables is the order of $\underset{\sim}{e}_B$ namely N , and the number of independent variables is likely to exceed this. Thus, to ensure compatibility of the conditions expressed by equations (4.3) and (4.4), the method of least squares is used to minimise the "error" between e_A and $\underset{\sim}{e}_B$; i.e. the product $\left[\underset{\sim}{e}_B - \underset{\sim}{e}_A\right]\left[\underset{\sim}{e}_B - \underset{\sim}{e}_A\right]^T$ is minimised. It can be readily shown that this leads to

$$\underset{\sim}{\delta} = \left[\underset{\sim}{H}^T\,\underset{\sim}{H}\right]^{-1}\underset{\sim}{H}^T\underset{\sim}{A}\,\underset{\sim}{q} \qquad (4.5)$$

in which $\underset{\sim}{H} \equiv \underset{\sim}{G}\,\underset{\sim}{F}^{-1}$. The overall strain energy in the jacks is then $\frac{1}{2}\,\underset{\sim}{\delta}^T\,\underset{\sim}{K}\,\underset{\sim}{\delta}$, where $K \equiv \text{diag}\left\{K_1,\ K_2,\ K_3\right\}$ represents the stiffnesses of the three control jacks.

The contributions to the stiffness coefficients are provided by the last term in equation (A.1.4.) and because $\underset{\sim}{G}$ and hence $\underset{\sim}{H}$ is periodic it is possible for these contributions to also be periodic. The individual blade motions are coupled together through the swashplate, and this is manifested by the appearance of coupling terms in the stiffness matrix.

It should be noted that since $\underset{\sim}{e}_A = \underset{\sim}{e}_B$ is identically possible, then the minimum value of the "error" product is zero.

4.2. Stability check

The presence of periodic coefficients in the equations of motion points to the possibility of parametric instability at certain rotor speeds (see Barr and Done [9]). As a preliminary check, a model was set up on AGEM consisting of a 4-bladed rotor having one fundamental flap and one fundamental pitch mode per blade. Aerodynamic forces were excluded, and the data relating to the blades and the jack and pitch control mechanism were those of the Lynx. The latter is of the spider-spindle type, rather than swashplate, and this has the effect of making the form of $\underset{\sim}{F}$ in

equation (4.1) somewhat simpler. It can then be shown that $\left[\underset{\sim}{H}^T \underset{\sim}{H}\right]$ in equation (4.5) is a diagonal matrix of scalar terms, and that periodic contributions appear in the structural stiffness matrix when the effective stiffnesses of the cyclic control jacks are unequal. This is in fact the case with the Lynx; it can further be easily demonstrated from the analysis that the periodic contributions vary at twice per rotor revolution.

A stability study on the 8 d.o.f. model was carried out for a range of rotor speeds up to $3\Omega_{op}$, where Ω_{op} is the normal operating speed, in increments of 0.05 Ω_{op} using the Floquet technique to obtain eigenvalues. Instabilities were detected at speeds of 0.2, 0.25, 1.25, 1.75 and 2.25 Ω_{op}. Below 0.2 Ω_{op} a clear solution could not be obtained. Bearing in mind that this model is completely undamped, and that it is a characteristic of parametric vibration that isolated instabilities are readily suppressed by the presence of only a small amount of damping, the effect was not considered important. Indeed, in extensive testing and operation of the Lynx overmany years, freedom from any such instabilities has been clearly demonstrated.

5. Discussion

This paper describes the work concerned with the development of the computer program AGEM subsequent to that reported in Refs [1] and [2]. The verification exercises used to explore the applicability and limitations of the program in the current work have centred on air resonance stability of the Lynx helicopter and the bearingless main rotor experimental model. The latter highlighted the importance of correctly modelling the system (in the mathematical sense), particularly in regard to split load paths and input data points. The other verification exercise concerned the incorporation of transmission system dynamics into the overall model. The inclusion of flexible fuselage dynamics can equally be performed without difficulty, but lack of results from other means of analysis meant that a full verification could not be carried out.

The latter two examples help illustrate the scope of the AGEM, and this is further demonstrated by Section 4 concerned with the effects of non-homogeneity in the (non-rotating) rotor control jack stiffnesses.

These exercises have allowed consolidation of experience and confidence in the use of AGEM. The program has been mounted and tested at WHL, Yeovil, since 1985 and is now running at RAE, Farnborough.

6. Acknowledgements

The authors would like to express their appreciation to Dr S P King of Westland Helicopters Ltd., and to Mr R J Davies and Mr W R Walker of the RAE, Farnborough, for their continued support and encouragement. This work was funded by the Ministry of Defence.

7. References

1. M P Gibbons and G T S Done. Automatic generation of helicopter rotor aeroelastic equations of motion. Vertica 8(3), 229-241 (1984). (Also: 8th European Rotorcraft and Powered Lift Aircraft Forum, 31 Aug-3 Sept 1982, Aix-en-Provence).

2. M H Patel and G T S Done. Experience with a new approach to rotor aeroelasticity. Vertica 9(3), 285-294 (1985). (Also: 10th European Rotorcraft Forum, 28-31 Aug 1984, The Hague).

3. P P Friedmann. Recent Developments in Rotary-wing Aeroelasticity J Aircraft, 14 (11), 1977.

4. P P Friedmann. Formulation and Solution of Rotary-wing Aeroelastic Stability and Response Problems. Vertica, 7 (2), 101-141 (1983).

5. D H Hodges, A S Hopkins, D L Kunz and H E Hinnant. Introduction to GRASP-General Rotocraft Aeromechanical Stability Program - a modern approach to rotocraft modelling. J Amer. Helicopter Soc., 32(2), 78-90 (1987).

6. Garrad A D and Quarton D C The Use of Symbolic Computing as a Tool in Wind Turbine Dynamics. Journal of Sound and Vibration, 109(1), 65-78 (1986).

7. A R S Bramwell. Helicopter dynamics. Edward Arnold, London (1976).

8. P T W Juggins. Substantiation of the analytical prediction of ground and air resonance stability of a bearingless rotor, using model scale tests. 12th European Rotorcraft Forum, 22-25 September 1986, Garmisch-Partenkirchen.

9. A D S Barr and G T S Done. Parametric oscillations in aircraft structures. Aeronautical Journal, 75, 654- 658, (1971).

Appendix A.1: Expressions for matrix coefficients

The full derivation for the expressions which appear below is given in Ref.[1]. The coefficients are the elements of the matrices [P], [Q] and [R] in the equations of motion:

$$[P]\ddot{\underline{q}} + [Q]\dot{\underline{q}} + [R]\underline{q} = \underline{0} \qquad .. \text{(A.1.1)}$$

in which $\underline{q}$ is a vector of generalised co-ordinates representing perturbations from some steady-state situation. The matrix coefficients are:

$$P_{ij} = \int \frac{\partial \underset{\sim}{R}}{\partial q_i} \cdot \frac{\partial \underset{\sim}{R}}{\partial q_j} dm \qquad .. \text{(A.1.2)}$$

$$Q_{ij} = 2\int \frac{\partial \underset{\sim}{R}}{\partial q_i} \cdot \frac{\partial^2 \underset{\sim}{R}}{\partial q_j \partial t} dm - \int \frac{\partial R}{\partial \underset{\sim}{q}_i} \cdot \frac{\partial \underset{\sim}{F}}{\partial \dot{q}_j} dS \qquad .. \text{(A.1.3)}$$

$$R_{ij} = \int \frac{\partial \underset{\sim}{R}}{\partial q_i} \cdot \frac{\partial^3 \underset{\sim}{R}}{\partial q_j \partial t^2}\, dm + \int \frac{\partial^2 \underset{\sim}{R}}{\partial q_i \partial q_j} \cdot \frac{\partial^2 \underset{\sim}{R}}{\partial t^2}\, dm \qquad .. \text{(A.1.4)}$$

$$- \int \frac{\partial \underset{\sim}{R}}{\partial q_i} \cdot \frac{\partial \underset{\sim}{F}}{\partial q_j}\, dS - \int \frac{\partial^2 \underset{\sim}{R}}{\partial q_i \partial q_j} \cdot \underset{\sim}{F}\, dS$$

$$+ \int \frac{\partial^2 U}{\partial q_i \partial q_j}\, dV$$

in which $\underset{\sim}{R}$ is the position vector of a point in the helicopter with reference to space fixed or inertial axes, $\underset{\sim}{F}$ is the aerodynamic force vector per unit area referred to the same axes, U is strain energy, dm is an elemental mass, dS an elemental area and dV an elemental volume. The integral signs are symbolic, the integration being as indicated by dm, dS or dV and over an appropriate extent, e.g. the total number of blades, the blade lifting surface, the fuselage, etc. The dot products ensure that the integrals are of scalar quantities. Structural damping is introduced into $[Q]$ separately.

To evaluate the integrals, $\underset{\sim}{R}$ and $\underset{\sim}{F}$ have to be expressed in terms of local co-ordinates by means of a set of transformations (see Appendix A.2); the differentials are performed numerically for a given time instant and the integrations (also numerical) are arranged so that, for a blade, they utilise blade properties expressed along a blade axis. The general scheme is explained in Ref.[1].

Appendix A.2: Formulation of transformation from local to fixed axes

Figs. 5(a) and (b) show the various deformations and axes that enable the transformation from local co-ordinates based on moving axes to co-ordinates based on fixed or inertial axes to be made. The flap, lag and twist deformations are expressed in terms of assumed modes, each of these being associated with a generalised co-ordinate, q_i. The assumed modes may be experimentally obtained or previously calculated, or based on some simple algebraic form, e.g. polynomial, trigonometric etc. Thus:

$$\left.\begin{aligned} f_\beta(s) &= \beta_o s + f_{\beta o}(s) + \sum_i f_{\beta i}(s) q_i \\ f_\zeta(s) &= \zeta_o s + f_{\zeta o}(s) + \sum_i f_{\zeta i}(s) q_i \\ \theta_s(s) &= \theta_o(s) + \theta_{os}(s) + \sum_i f_{\theta i}(s) q_i \end{aligned}\right\} \qquad .. \qquad .. \text{(A.2.1)}$$

in which $f_\beta(s)$, $f_\zeta(s)$ and $\theta_s(s)$ are the flap, lag and pitch deflections at a station distance s along the blade axis, β_o is the coning angle, ζ_o the steady lag, and θ_o the combined built-in twist

and applied pitch. The sectional steady-state values are given by $f_{\beta o}(s)$, $f_{\zeta o}(s)$ and $\Theta_{os}(s)$, and the contributions from each mode q_i are $f_{\beta i}(s)$, $f_{\zeta i}(s)$ and $f_{\theta i}(s)$. Any mechanical pitch/flap or pitch/lag coupling terms (i.e. due to δ_3 and α_2), and collective and cyclic pitch (e.g. arising from the ASE) is inserted into the expression for $\Theta_s(s)$. Differentiation of $f_\beta(s)$ and $f_\zeta(s)$ with respect to s provides expressions for local flap and lag angles, $\beta(s)$ and $\zeta(s)$ respectively. Further angles, necessary to formulate rotation transformation matrices are $T \equiv \Omega t$ (instantaneous angle of rotation of the datum blade about the rotor axis), η (rotor axis tilt), and ϕ, ψ, γ (fuselage roll, pitch and yaw).

It can be shown that a point at $\underset{\sim}{r}_{10} \equiv \{x_{10}, y_{10}, z_{10}\}$ on a blade (local blade axes with $x_{10} = 0$, see Fig. 5(a)) may be expressed in terms of axes attached to the rotor hub as

$$\underset{\sim}{r}_h \equiv \{x_5, y_5, z_5\}$$

$$= [A_1]\underset{\sim}{r}_{10} + \underset{\sim}{B}_1 \qquad .. \qquad .. \qquad .. \qquad .. \quad (A.2.2)$$

where $[A_1] = [T_T][T_\beta][T_\zeta][T_\theta]$

$$[B_1] = [T_T](\underset{\sim}{r}_6 + [T_\beta]\underset{\sim}{r}_5)$$

$$\underset{\sim}{r}_5 = \begin{bmatrix} -\frac{1}{2}\int_0^s \zeta(s)^2 ds \\ f_\zeta(s) \\ 0 \end{bmatrix}$$

$$\underset{\sim}{r}_6 = \begin{bmatrix} s - \frac{1}{2}\int_0^s \beta(s)^2 ds \\ Y_0 \\ Z_0 + f_\beta(s) \end{bmatrix}$$

in which Y_0 and Z_0 define the built-in blade axis offset. A rotational transformation matrix is denoted $[T_{(angle)}]$; the angle indicates the angle between the axes concerned. A typical matrix is, for example:

$$[T_\theta] = \begin{bmatrix} 1 & 0 & 0 \\ 0 & \cos\Theta(s) & -\sin\Theta(s) \\ 0 & \sin\Theta(s) & \cos\Theta(s) \end{bmatrix}$$

The diagonal positioning of the 'one' depends upon the axes about which the rotational transformation is taking place.

For axes fixed in space:

$$\underset{\sim}{r}_0 \equiv \{x_0, y_0, z_0\}$$

$$= [A]\underset{\sim}{r}_{10} + \underset{\sim}{B} \qquad .. \qquad .. \qquad .. \qquad .. \quad (A.2.3)$$

where $[A] = [T_\gamma][T_\psi][T_\phi][T_\eta][A_1]$

$$\underset{\sim}{B} = [T_\gamma][T_\psi][T_\phi]([T_\eta]\underset{\sim}{B}_1 + \underset{\sim}{r}_{ac}) + \underset{\sim}{r}_f$$

in which $\underset{\sim}{r}_{ac}$ defines the co-ordinates of the aircraft centre of mass, and $\underset{\sim}{r}_f \equiv \{q_{xf}, q_{yf}, q_{zf}\}$ is a vector of the fuselage translational displacements (see Fig. 5(b)). The suffices η, Φ, Ψ and γ refer to rotor shaft tilt, and fuselage roll, pitch and yaw respectively. It is normally convenient to align the $\underset{\sim}{r}_0$ axes with the instantaneous position of the fuselage principal axes.

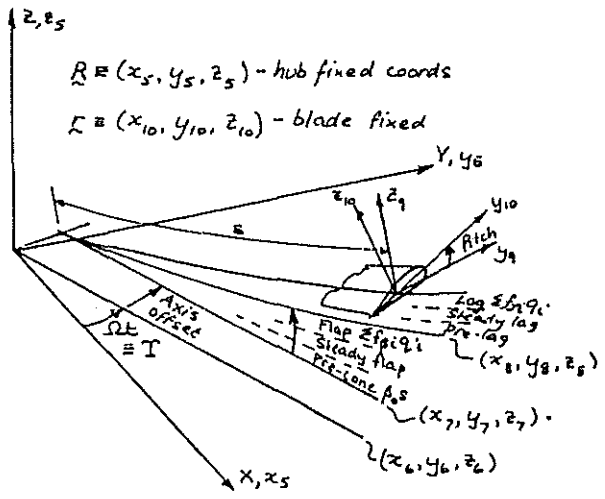

Fig.5(a): Transformations to hub-fixed axes

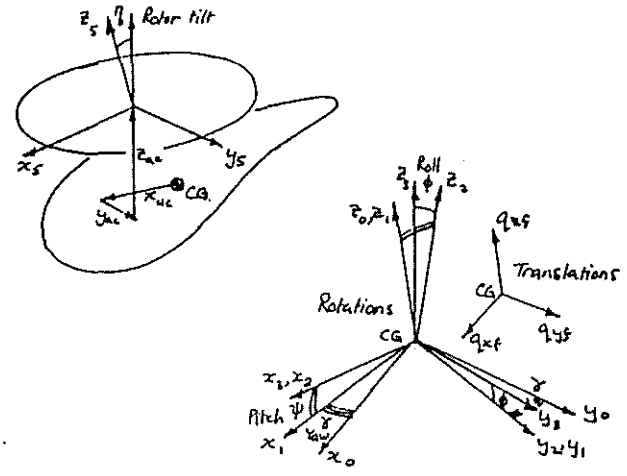

Fig.5(b): Transformations to space-fixed axes

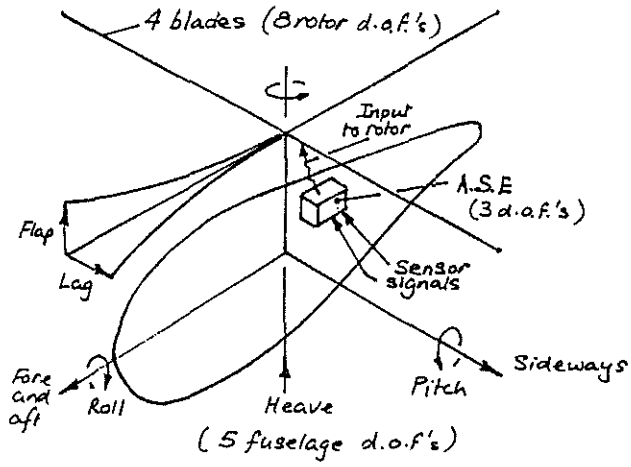

FIG 1 AIR RESONANCE MODEL

Table 1: Real and imaginary parts of eigenvalues, air resonance in forward flight.

WHL results		*AGEM results*	
Real	*Imaginary*	*Real*	*Imaginary*
-0.0199	9.48	-0.0199	9.49
-0.064	7.34	-0.056	7.43
-2.589	10.88	-2.70	10.88
-2.433	10.88	-2.34	10.88
-0.076	3.54	-0.065	3.54
-2.32	5.50	-2.28	5.49
-2.58	5.49	-2.60	5.5
-0.0431	1.87	-0.038	1.87
-0.191	1.35	-0.188	1.34
-2.56	1.32	-2.56	1.31
-2.27	0.798	-2.20	0.69
-0.195	0.627	-0.193	0.63
-0.296	0.096	-0.32	0.15
-0.111	0	-0.11	0
-0.007	0	-0.01	0
-0.0326	0	-0.048	0

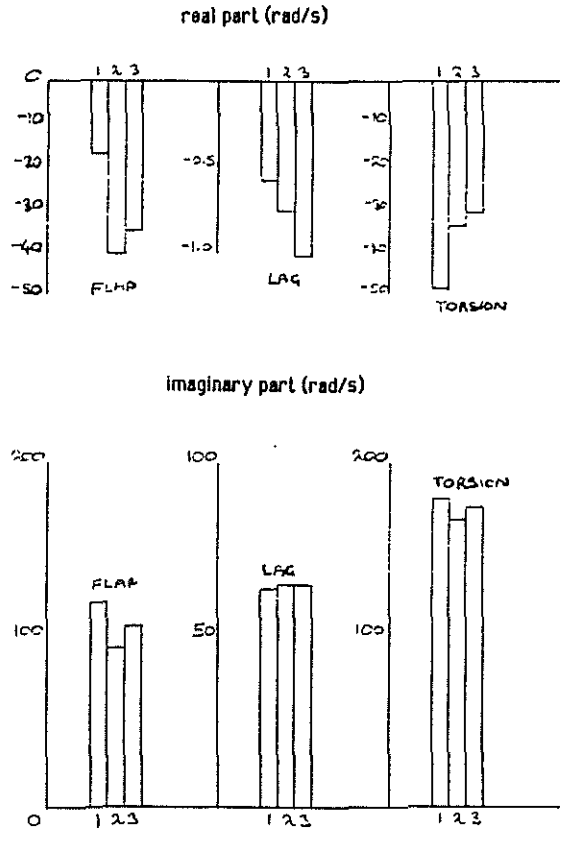

Cases:
1 Result from WHL program J133
2 AGEM with no torque tube representation
3 AGEM with torque tube representation

Fig 2 Calculated eigenvalues for model BMR: comparison of single-blade hub-fixed cases (3 coupled blade modes)

Table 2: Comparison of natural frequencies when the transmission system is included.

Natural frequency Hz	
WHL	*AGEM*
5.39	5.40
7.82	7.91
16.6	16.6
18.9	18.95
36.3	38.0
63.6	69.5

Table 3: Natural frequencies for flexible fuselage model with and without rotor flexibility.

Flexible fuselage with lumped mass rotor		*Flexible fuselage with flexible rotor*
Description of main rotor head motions	*Natural frequency Hz*	*Natural frequency Hz (fuselage modes)*
Fore/aft and heave	13.792	14.33
Fore/aft	18.466	18.56
Fore/aft and roll	18.783	19.67
Sideways	19.170	20.00
Sideways, roll and yaw	30.19	32.32
Yaw	35.445	*

* No comparable frequency obtained.

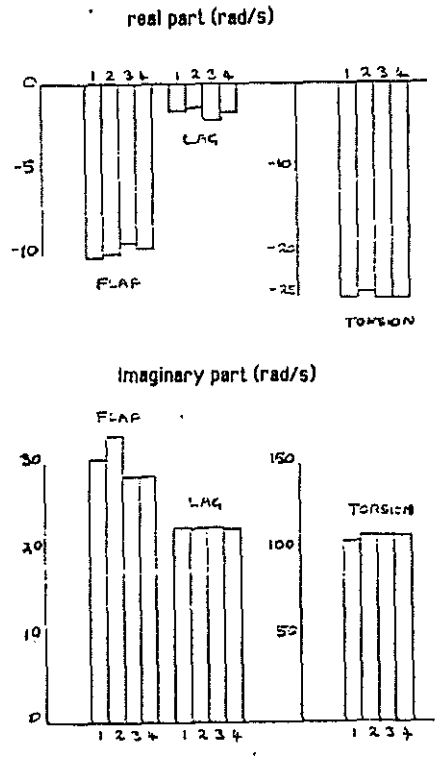

Cases:
1 Result from WHL program J133
2 AGEM with sparse points around control load path branch
3 AGEM with internally computed structural stiffness
4 AGEM with externally computed structural stiffness

Fig3 Calculated eigenvalues for 'theoretical' rotor: comparison of single-blade hub-fixed cases (3 coupled blade modes)

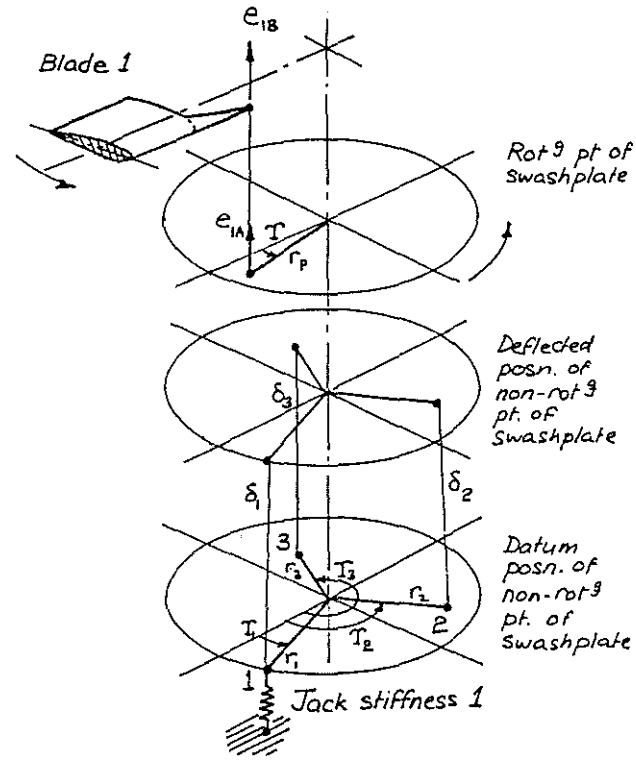

FIG 4. ROTOR PITCH CONTROL THROUGH SWASHPLATE